HHS Public Access

Author manuscript

J Immunol. Author manuscript; available in PMC 2017 January 15.

Published in final edited form as:

J Immunol. 2016 January 15; 196(2): 726–737. doi:10.4049/jimmunol.1501266.

Targeting of Ly9 (CD229) disrupts marginal zone and B1 B cell homeostasis and antibody responses[1]

Marta Cuenca[*], **Xavier Romero**[*], **Jordi Sintes**[*], **Cox Terhorst**[†], and **Pablo Engel**[*]

[*]Immunology Unit, Department Cell Biology, Immunology and Neurosciences, Medical School, University of Barcelona, Barcelona, Spain

[†]Division of Immunology, Beth Israel Deaconess Medical Center, Harvard Medical School, Boston, USA

Abstract

Marginal zone and B1 B-cells have the capacity to respond to foreign antigens more rapidly than conventional B-cells, providing early immune responses to blood-borne pathogens. Ly9 (CD229, SLAMF3), a member of the SLAM family receptors, has been implicated in the development and function of innate T lymphocytes. Here, we provide evidence that in Ly9-deficient mice splenic transitional T1, marginal zone and B1a B cells are markedly expanded, whilst development of B lymphocytes in bone marrow is unaltered. Consistent with an increased number of these B cell subsets, we detect elevated levels of IgG3 natural antibodies, and a striking increase of T-independent type II antibodies following immunization with TNP-Ficoll in the serum of Ly9-deficient mice. The notion that Ly9 could be a negative regulator of innate-like B cell responses was supported by the observation that administering a mAb directed against Ly9 to WT mice selectively eliminated splenic marginal zone B cells and significantly reduced the numbers of B1 and transitional T1 B cells. Additionally, Ly9 mAb dramatically diminished *in vivo* humoral responses and caused a selective down-regulation of the CD19/CD21/CD81 complex on B cells and concomitantly an impaired B cell survival and activation in a Fc-independent manner. We conclude that altered signaling due to the absence of Ly9 or induced by anti-Ly9 may negatively regulate development and function of innate-like B cells by modulating B cell activation thresholds. The results suggest that Ly9 could serve as a novel target for the treatment of B cell related diseases.

Introduction

Marginal zone (MZ) and B1 B cells are distinct B lymphocyte subsets that differ from conventional follicular B cells both developmentally and functionally. These two cell types have been termed innate B lymphocytes since they share many properties with innate

[1]This work was supported by the Ministerio de Educación y Ciencia through grants SAF2012-39536 (P.E.) and a grant from the National Institutes of Health PO1 AI 065687 (to C.T. and P.E.). M.C. was supported by Ministerio de Educación, Cultura y Deporte (AP2010-1754).

Corresponding author: Pablo Engel, Immunology Unit. Department Cell Biology, Immunology and Neurosciences. Medical School. University of Barcelona. Casanova 143, Barcelona 08036, Spain, pengel@ub.edu; Phone No. +34 93 2275400 (ext 4010).

Conflict of interest disclosure

The authors have no conflicts of interest to disclose.

immune cells, and serve as a bridge between the rapidly occurring innate responses and the slower adaptive immunity (1). Because of their anatomical location, MZ and B1 B cells are the earliest lymphocytes to encounter invading viruses and bacteria acquired through the blood stream and the gut/peritoneum. These B cell subsets have evolved to provide a first line of defense against pathogens by mounting quick and potent humoral responses, characterized by the production of antibodies with a broad reactivity (2). They play an important role in T-independent antibody responses, particularly to T-independent type II (TI-2) antigens (3). Antibody responses to these antigens are essential for generating protective immunity against the cell-wall polysaccharides expressed by a number of capsulated bacterial pathogens, such as *Streptococcus pneumoniae* (4). Despite numerous insights into the understanding of these humoral responses, the molecular mechanisms regulating TI-2 Ag responses and MZ and B1 B cells homeostasis remain only partially understood (5).

Leukocyte cell-surface molecules are required for the appropriate development, activation and effector functions of lymphocytes. Most of these transmembrane molecules mediate adhesion and elicit intracellular signals that positively or negatively regulate immune responses. Among the different families of cell-surface molecules, the signaling lymphocytic activation molecule (SLAM) family receptors have been shown to exert crucial immunomodulatory functions in the regulation of several immunological processes such as lymphocyte development and survival, cytotoxicity, cell adhesion and humoral immunity (6, 7). Recently, several reports have demonstrated that the SLAMF receptors are crucial to the development of innate-like T lymphocytes, such as *i*NKT cells (8, 9).

Ly9, also known as CD229 or SLAMF3, is one of the nine members of the SLAM family. It is expressed on all T and B lymphocytes (10). Interestingly, its highest expression levels are found on innate-like lymphocytes such as *i*NKT cells and MZ B cells (11). Ly9 is also expressed in virtually all chronic lymphocytic leukemias (CLL) (12). Its expression is not lost during B cell differentiation into plasma cells, and it is highly expressed on multiple myeloma cells (13). Ly9 has four extracellular Ig-like domains, and as has been shown with other SLAMF members, the N-terminal Ig domain of Ly9 mediates homophilic adhesion (14). Its cytoplasmic tail contains two copies of the conserved tyrosine-based switch motif (ITSM), which is a docking site for the adapter molecules SLAM-associated protein (SAP) and Ewing's sarcoma-associated transcript 2 (EAT-2), and also for phosphatases such as SHIP and SH2 domain-containing phosphatase (SHP-2) (15, 16). Recently, we have shown that in contrast to SLAMF1 and SLAMF6, Ly9 has a negative rather than a positive role in the signaling pathways required for *i*NKT development and innate-like CD8 T cell expansion in the thymus (17). Moreover, aged Ly9-deficient mice spontaneously develop features of systemic autoimmunity, such as splenomegaly and production of autoantibodies, indicating that the Ly9 cell-surface receptor is involved in the maintenance of immune cell tolerance (18). All these data support the view that Ly9 differs from the other SLAMF members by acting as a non-redundant inhibitory molecule. To date, however, the regulatory effects of Ly9 on B cell biology remain elusive.

Our main goal was to elucidate the function of Ly9 in B cell development and homeostasis. This study demonstrated that Ly9 negatively regulates innate B lymphocyte homeostasis and

function. Importantly, it also shows that antibody-mediated targeting of Ly9 hampers B cell responses.

Methods

Mice

Wild-type (WT) BALB/c and C57BL/6 mice were obtained from Charles River Laboratories (Saint-Aubin-lès-Elbeuf, France). $Ly9^{-/-}$ (129 x B6) mice, kindly provided by Dr. McKean (19), were backcrossed to BALB/c or C57BL/6 backgrounds for at least 12 generations. All animals were used at 8–12 wk of age, and housed under specific pathogen-free conditions.

Immunizations

Mice were immunized intraperitoneally with 100 μg of 2,4,6-trinitrophenyl (TNP)-keyhole limpet hemocyanin (KLH) conjugate (TNP_{31}-KLH; Biosearch Technologies) in complete Freund's adjuvant (Sigma) at day 0, and boosted at day 14 with 100 μg TNP_{31}-KLH diluted in PBS. For assessment of T-Independent responses, mice received i.p. 50 μg $TNP_{0.3}$-LPS or 50 μg TNP_{65}-Ficoll (Biosearch Technologies) in PBS. Serum samples were collected from the tail vein at the indicated time points after immunization.

ELISAs

For the detection of TNP-specific antibodies, high binding plates (Costar) were coated with 4 μg/ml TNP_{18}-BSA (Biosearch Technologies) diluted in PBS. For the detection of natural antibodies, plates were coated with either 8 μg/ml Pneumo23® vaccine (Sanofi Pasteur) or 5 μg/ml PC_{16}-BSA (Biosearch Technologies) in PBS. For the detection of total IgG or IgM levels in serum, plates were coated with 3 μg/mL anti-mouse IgG (Sigma) or 3 μg/mL F(ab′)$_2$ fragments anti-IgM (Jackson Immunoresearch). Serum samples were added at an optimal dilution chosen from a previous titration curve. Bound antibodies were detected using either anti-mouse IgG peroxidase (Sigma), or biotin-conjugated goat anti-mouse IgM, IgG1, IgG2a, IgG2b, and IgG3 (Jackson Immunoresearch) and streptavidin-peroxidase (Roche). Plates were developed with o-Phenylenediamine dihydrochloride (OPD) (Sigma), and read on an Epoch plate reader at 405 nm.

Flow cytometry

Cell suspensions of lymphocytes from spleen, blood, peritoneum, and bone marrow were treated with red blood cell lysis buffer (0.15M NH_4Cl, 0.01M TrisHCL), washed and incubated in 20% heat-inactivated rabbit serum before being stained with fluorophore-labelled antibodies. The following anti-mouse monoclonal antibodies were purchased from BD Pharmingen: CD11b-PE and FITC (M1/70), CD21/CD35-FITC (7G6), CD23-PE (B3B4), CD43-FITC (S7), CD86-PE (GL1), CXCR5-biotinylated (2G8), IgM-biotinylated (R6-60.2), and TNP-PE (G235). The mAbs B220-PB and APC (RA3-6B2), CD11c-PECy7 (N418), CD19-A647 (6D5), CD69-PerCP (H1.2F3), CD81-PE (EAT-2), CD138-PECy7 (281-2) and integrin beta 7-APC (FIB504) were obtained from Biolegend. CD5-PECy7 (53-7.3), CD62L-APC (MEL-14), CD93-PerCP-Cy5.5 (AA4.1) and SIGN-R1-APC (eBio22D1) were purchased from eBioscience. Anti-mouse CD49d (integrin alpha 4) VioBlue (R1-2) and MHC-II FITC (REA528) were obtained from Miltenyi Biotec. Anti-

mouse S1P1-APC (713412) was purchased from R&D Systems; anti-mouse CD18-FITC (C71/16) was from Sigma ImmunoChemicals; biotinylated anti-MOMA-1 was from Abcam. The antibodies anti-mouse IgM-FITC (polyclonal) and IgD-PE (11-26c) were obtained from SouthernBiotech. Streptavidin Brilliant Violet 421 and Streptavidin PECy5 were obtained from Biolegend. Data was acquired with FACSCanto II cytometer and analyzed with FlowJo software (TreeStar).

In vitro stimulation assays

Spleen single-cell suspensions were depleted of red blood cells and cultured in RPMI media supplemented with 10% FCS, 2μM L-glutamine, 50 U/mL penicillin, and 50 μg/mL streptomycin. Cells were stimulated with goat $F(ab')_2$ anti-IgM (10 μg/mL, Jackson Immunoresearch) for 6h, and upregulation of activation markers was assessed by flow cytometry.

MZ B cell isolation and phospho-flow analysis

Marginal zone B cells were purified with the Marginal Zone and Follicular B Cell isolation kit (Miltenyi Biotec) following manufacturer's protocol. For the assessment of BCR signaling events, cells were simulated for 5 minutes in the presence of 10 μg/mL $F(ab')_2$ anti-IgM (Jackson Immunoresearch). After the incubation time, cells were fixed immediately by adding 3% formaldehyde directly into the culture medium to obtain a final concentration of 1.5% formaldehyde. Cells were incubated in this fixation buffer for 10 minutes at 37°C and then pelleted. Cells were permeabilized with ice-cold Perm Buffer III (BD) at 4°C for 30 minutes, then washed in FACS wash buffer (PBS with 2%FCS and 0.01% NaN3) and resuspended in staining buffer. The detection of phosphorylated epitopes was carried out by using the mAbs Btk(pY223)-A647 (N35-86), JNK(pT183/pY185)-PE (N9-66), and p38 (pT180/pY182)-PE (36/p38), all from BD.

Tissue staining and confocal microscopy

Wild-type BALB/c mice received 250 μg i.p. of Ly9.7.144 or control antibody (IgG1). Twenty-four hours later, spleens were collected and frozen in Tissue-Tek® OCT Compound (Sakura). Five μm sections were cut in a cryostat microtome (Leica). Slides were fixed in acetone and stored at −80°C. Before staining, samples were extensively washed with PBS and blocked with 6% fetal bovine serum in PBS during 30 minutes at room temperature. Endogenous biotin was blocked by using an Avidin/Biotin blocking kit (Vector Laboratories) following the manufacturer's protocol. Samples were incubated overnight at 4°C with anti-mouse IgM-FITC (polyclonal; SouthernBiotech), anti-SIGN-R1-APC (clone eBio22D1; eBioscience), biotinylated anti-MOMA-1 (MOMA-1; Abcam), biotinylated anti-VCAM-1 (Caltag), or anti-ICAM-1 PE (3E2; BD) followed by incubation with AlexaFluor 555® conjugated streptavidin (Life technologies) or anti-hamster rhodamine (Jackson Immunoresearch). Laser Scanning Confocal images were acquired using a Leica TCS SL laser scanning confocal spectral microscope (Leica Microsystems) equipped with Argon and HeNe lasers and a Leica DMIRE2 inverted microscope. FITC, Alexa555 and APC emission were acquired sequentially with a triple dichroic beam-splitter (TD 488/543/633nm); excitation at 488/543/633 nm and emission detection ranges: 500–540 nm, 555–625nm, 643–700 nm, respectively. Images were obtained using HCPLFLUOTAR10x Dry

(numerical aperture, NA 0.3), HCPLFUOTAR 20x Dry objective lens (NA 0.5) equipped with phase contrast optics and the confocal pinhole set at 1 Airy unit. Image assembly, processing and quantification were performed using ImageJ software.

TNP-Ficoll capture in the MZ

Ly9$^{-/-}$ and age-matched wild-type mice were injected intravenously with 50 μg of TNP_{65}-Ficoll (Biosearch Technologies). After 30 minutes, TNP binding to spleen B cells was assessed by flow cytometry. Distribution of TNP^+ cells was assessed by immunofluorescent analysis; tissues were processed as described above and stained with antibodies against TNP, IgM, and SIGN-R1.

In vivo treatment with Ly9.7.144

For analysing spleen B cell subsets, BALB/c mice received i.p. 250 μg of Ly9.7.144 (IgG1) monoclonal antibody, generated in our laboratory (17), or an isotype control (IgG1) mAb diluted in PBS. $F(ab')_2$ were generated using the Pierce™ Mouse IgG1 Fab and $F(ab')_2$ Micro Preparation Kit (Thermo Scientific). Spleen, blood and bone marrow populations were analysed by FACS either 1 or 26 days later. To assess humoral responses after anti-Ly9 treatment, BALB/c or CD1d$^{-/-}$ mice were i.p. injected with 250 μg Ly9.7.144 or 250 μg mouse IgG1 control 24h before being immunized with T-D, TI-1 and TI-2 antigens as described above. To assess $F(ab')_2$ Ly9.7.144 *in vivo* effects on B cell populations, BALB/c mice received i.p. 50 μg of whole Ly9.7.144, $F(ab')_2$ Ly9.7.144, or isotype control mAb. Twenty-four hours later, spleen B subsets were analysed by FACS. For analysis of TI-2 responses after treatment with $F(ab')_2$ Ly9.7.144 fragments, BALB/c mice received 50 μg of Ly9.7.144, $F(ab')_2$ Ly9.7.144 or isotype control mAb i.p. on days 0, 3, and 6. On day 1, mice were immunized i.p. with 50 μg TNP_{65}-Ficoll in PBS. On day 8, mice were sacrificed and anti-TNP specific antibody levels in the serum were determined by ELISA as described above.

Ex vivo analysis of proliferation, viability and IgG production of anti-Ly9 treated cells

BALB/c mice received i.p. 250 μg of Ly9.7.144 or IgG1 control mAb. Twenty-four hours later, spleen lymphocytes were isolated and stained with CellTrace™ CFSE (Life Technologies) following manufacturer's instructions. A total of 10^6 lymphocytes were cultured in 0.5 mL of complete RPMI in 24-well plates. Cells were cultured for 72h in medium alone or in the presence of 10 μg/mL LPS (Sigma), or 10 μg/mL $F(ab')_2$ anti-mouse IgM (Jackson ImmunoResearch). Viability was assessed by staining with Live/Dead Fixable far red dye (Invitrogen) following the manufacturer's protocol.

IgG levels in the supernatants were determined by ELISA. 96-well plates were coated with 3 μg/mL anti-mouse IgG (Sigma). A purified in-house mouse IgG antibody was used as a standard. Bound IgG was detected with peroxidase-conjugated anti-mouse IgG (Sigma). The reaction was developed with OPD substrate (Sigma) and read at 405 nm.

Statistical analysis

Differences between group means were assessed with GraphPad Prism 5, using unpaired two-tailed Student *t* tests unless otherwise indicated. The paired *t* test was used to compare Ig levels on each mouse before and after anti-Ly9 treatment.

Results

Significantly higher numbers of splenic T1 Transitional, MZ, B1 B cells and consequently increased production of natural antibodies in Ly9-deficient mice

Analysis of B cell development in Ly9-deficient ($Ly9^{-/-}$) mice showed no major alterations in bone marrow B cell subsets (data not shown). In contrast, the absence of Ly9 led to an expansion of splenic $B220^+$ B cells compared to WT mice, both in percentages and absolute numbers (62.18% ± 1.07 vs. 52.87% ± 0.62; p>0.0001; 71.92±4.18 vs. 53.18±2.68 cell numbers $x10^6$). This increase was also observed in the proportion of mature B cells in blood, lymph node, and bone marrow (data not shown). The most striking finding, however, was a marked expansion, approximately two-fold, of transitional and MZ B cells in the spleen of $Ly9^{-/-}$ mice (Fig. 1). The increase in transitional B cells ($B220^+$ $CD93^+$) was due to an expansion of T1, but not T2 or T3, cells (Fig. 1A–C). Moreover, analysis of the mature B lymphocytes showed an increase in B1 cells (Fig. 1G–I). B1 cells were further subdivided into B1a and B1b cells, based on CD5 expression, showing that the increase in splenic B1 cells resulted from an expansion of B1a, but not B1b, cells (Fig. 1H, 1I). Surprisingly, no significant alterations in the peritoneal B1 cell populations were detected (data not shown). In conclusion, our results show that the absence of Ly9 promotes an expansion of innate-like B cells subsets in the spleen.

To gain insight into the nature of innate-like B cells expansion in the absence of Ly9, we decided to analyze the expression of various activation markers on splenic B cell subsets of $Ly9^{-/-}$ and WT mice, before and after BCR cross-linking. Ly9-deficient MZ and B1 B cells displayed higher expression of MHC-II in basal conditions, whereas $Ly9^{-/-}$ FO B cells presented normal levels (Supplemental Fig. 1A). These higher levels of MHC class II suggested that Ly9-deficient innate-like B cells had the potential to respond more potently to activating signals. However, no significant differences were seen in the viability and proliferation rate of Ly9-deficient B cells after 24h of stimulation with anti-IgM or LPS (data not shown). Since BCR signaling strength influences the differentiation of transitional B cells into MZ or FO B cells, we examined signaling events downstream of the BCR in isolated MZ B cells from WT and $Ly9^{-/-}$ mice. Interestingly, Ly9-deficient MZ B cells expressed higher phosphorylation of Btk compared to WT cells, although this difference did not reach statistical significance (Supplemental Fig. 1B). After anti-IgM stimulation, upregulation of pBtk, pJNK, and pp38 in Ly9-deficient MZ B cells was similar to the observed in WT mice cells (Supplemental Fig. 1B), indicating that Ly9 absence does not significantly impair early BCR signaling events.

As MZ B cells and B1a cells are known to be the major source of natural antibodies in the absence of previous antigen contact, we assessed whether the serum levels of this antibody type were altered in Ly9-deficient mice. We tested the levels of IgM and IgG3, which are

the predominant subclass of natural antibodies, reactive with the Pneumo23® vaccine and phosphorylcholine (PC). Pneumo23® vaccine is composed of a mixture of 23 purified capsular polysaccharides from *Streptococcus pneumoniae*. Our results show a significant increase of IgG3 natural antibodies in Ly9-deficient mice compared with WT mice (Fig. 1J, 1K). No differences in IgM levels could be observed in either group of mice. Taken together, the data indicate that the presence of Ly9 prevents expansion of MZ and B1 cells.

Enhanced antibody responses against T-Independent type II antigens in Ly9-deficient mice

The observed alterations in B cell subsets in the absence of Ly9 prompted us to assess the role of Ly9 in the regulation of B cell function. To this end, we compared the response of WT and $Ly9^{-/-}$ mice to T-Dependent (TNP_{31}-KLH), T-Independent type I ($TNP_{0.3}$-LPS), and T-Independent type II (TNP_{65}-Ficoll) antigens. The absence of Ly9 did not impair antibody production against T-D or TI-1 antigens (Supplemental Fig. 2A, 2B). In contrast, TI-2 responses were enhanced in $Ly9^{-/-}$ mice. Upon TNP-Ficoll immunization, the serum of $Ly9^{-/-}$ BALB/c mice contained significantly higher levels of TNP-specific IgG2a, IgG2b and IgG3 compared with those of their WT counterparts (Fig. 2). Similarly, serum anti-TNP IgG levels were significantly increased after TNP-Ficoll immunization of $Ly9^{-/-}$ C57BL/6 mice as compared to WT animals (data not shown). These data support the concept that the Ly9 receptor negatively regulates TI-2 B cell responses independently of the genetic background. Taken together these data demonstrate that Ly9 functions as a negative regulator of T-independent humoral responses.

Marginal zone architecture and antigen capture is not altered in Ly9 absence

Marginal zone B cells retention and survival in the MZ is influenced by the structural framework and the survival signals delivered by MZ-related stromal and myeloid cells. We sought to determine if the increased numbers of MZ B cells in $Ly9^{-/-}$ mice were due to alterations of the splenic MZ architecture caused by Ly9 absence. Thus, we analyzed the frequency and location of myeloid subsets and the expression of adhesion molecules in the spleens of $Ly9^{-/-}$ mice. Cell numbers of plasmacytoid dendritic cells (pDCs) ($B220^+$ $CD11c^+$), conventional dendritic cells (cDCs) ($B220^-$ $MHC\text{-}II^+$ $CD11c^+$), $CD8^+$ cDCs ($B220^-$ $MHC\text{-}II^+$ $CD11c^+$ $CD8^+$ $CD11b^-$) and $CD11b^+$ cDCs ($B220^-$ $MHC\text{-}II^+$ $CD11c^+$ $CD8^-$ $CD11b^+$) were not altered in $Ly9^{-/-}$ spleens (Fig. 3A). Similarly, numbers of $MOMA\text{-}1^+$ metallophilic macrophages and $SIGN\text{-}R1^+$ MZ macrophages were normal in Ly9 absence (Fig. 3B). Tissue immunofluorescence analysis confirmed that $Ly9^{-/-}$ mice display a normal distribution of $MOMA\text{-}1^+$ and $SIGN\text{-}R1^+$ MZ macrophages (Supplemental Fig. 3A). Moreover, Ly9 deficiency did not lead to alterations in $VCAM\text{-}1^+$ endothelial cells or $ICAM\text{-}1^+$ marginal sinus cells in the MZ (Supplemental Fig. 3B).

As Ly9-deficient mice display enhanced T-independent type II antibody responses, we evaluated the ability of $Ly9^{-/-}$ MZ B cells and $SIGN\text{-}R1^+$ macrophages to capture TI-II blood borne antigens. WT and $Ly9^{-/-}$ mice received an i.v. injection of TNP-Ficoll, and 30 minutes later, we examined TNP^+ cells distribution. Immunofluorescence analysis of spleen sections stained with IgM, SIGN-R1 and TNP revealed that MZ B cells bound more TNP-Ficoll than did FO B cells, and TNP^+ cells were located mostly in the MZ. The distribution of TNP^+ cells in $Ly9^{-/-}$ mice was similar to the observed in their WT counterparts (Fig. 3C).

To corroborate these observations, we performed FACS analysis to quantify antigen uptake by MZ B cells. Ly9-deficient cells were able to trap TNP-Ficoll as efficiently as WT MZ B cells did, as judged by TNP MFI (Fig. 3D, 3E).

Taken together, these data suggest that both the increased antibody response against T-independent type 2 antigens and the expansion of MZ and B1 B cells observed in $Ly9^{-/-}$ mice are driven by a B-cell intrinsic mechanism triggered in Ly9 absence, rather than being a consequence of an altered splenic architecture.

Administering a monoclonal antibody directed against Ly9 selectively depletes splenic MZ and B1 B cells

To further explore the role of Ly9 in the humoral immune response, we produced a mouse monoclonal antibody directed against mouse Ly9 (Ly9.7.144) (Supplemental Fig. 4A, 4B). Upon administering this non-cytotoxic IgG1 mAb, MZ B cells could not be detected in WT BALB/c mice (Fig. 4A–C). Secondly, 24-hour after injecting anti-Ly9 the number of splenic B1 B cells was reduced by half (Fig. 4D–F). This depletion was selective, because anti-Ly9 did not affect other B lymphocyte subsets, *e.g.* follicular B cells (FO), even though they express high levels of Ly9 (Supplemental Fig. 4C). The slight increase in the percentage of FO B cells was most likely due to the reduction in the proportion of MZ B cells (Fig. 4A–C). Further evidence for the specific effect of the Ly9.7.144 mAb came from the observation that its administration to $Ly9^{-/-}$ mice did neither alter MZ nor B1 B cell numbers (Fig. 4A, 4D). Consistent with the flow cytometry analyses, a significant reduction in IgM^{+} B cells located in the MZ was observed in spleen tissue sections of anti-Ly9-treated mice (Fig. 4G). Elimination of MZ B cells caused by Ly9.7.144 was further confirmed by the absence of $CD1d^{hi}$ $CD23^{lo}$ lymphocytes in the spleen (data not shown). Interestingly, no effect on B1 cells in the peritoneal cavity was observed (data not shown). Because $CD21^{hi}$ $CD23^{lo}$ cells were not detected in the peripheral blood at 4 and 24h after administering anti-Ly9 (Fig. 4H, 4I), we reasoned that MZ B cells had been depleted rather than migrating into the bloodstream.

We further assessed the long-term effects of a single injection of 250 μg of anti-Ly9 antibody. 26 days after a single anti-Ly9 dose the numbers of T1 transitional B cells were reduced. Higher numbers of T2 and T3 transitional B cells were found, concomitant with the decrease in T1 transitional B cells (Fig. 5A, 5B). MZ B cells were still absent after 26 days (Fig. 5C, 5D), and a significant reduction in the percentage and absolute number of B1 cells was also maintained (Fig. 5E, 5F).

Moreover, levels of total serum IgM and IgG decreased approximately a 40% (Fig. 5G). Although $B220^{int}$ $CD138^{hi}$ plasma cells in the spleen were not affected, the number of plasma cells in the bone marrow was significantly reduced after this time (Fig. 5H). Thus, anti-Ly9 negatively regulates the number of innate-like B lymphocytes.

Pretreatment with anti-Ly9 reduces humoral responses

Because anti-Ly9 treatment caused a severe decrease in MZ zone and B1 cells, which are involved in T cell independent (T-I) antibody responses, we next analyzed the response to

TNP_{65}-Ficoll antigen in mice pretreated with Ly9.7.144 mAb. Injection of Ly9.7.144 caused a significant reduction in hapten-specific antibody production against TNP_{65}-Ficoll. This treatment affected all tested isotypes except IgM (Fig. 6A).

Remarkably, anti-Ly9 administration also reduced the levels of anti-TNP IgG1, IgG2a, IgG2b and IgG3 following immunization with T-D and TI-1 antigens (Fig. 6B, 6C). Since NKT cells have been shown to play a role in T-Dependent responses, and we have previously reported that Ly9 influences NKT development in the thymus (17), we sought to assess if the impaired antibody production against T-D antigens was due to the effect of Ly9.7.144 over NKT cells. To this end, we determined humoral response against TNP_{31}-KLH in NKT-deficient $CD1d^{-/-}$ mice pretreated with either anti-Ly9 or a control antibody. Ly9.7.144 administration dampened the production of TNP-specific IgG1, IgG2b, IgG3, and IgM in $CD1d^{-/-}$ mice (Fig. 6D), demonstrating that Ly9 targeting is able to impair T-D responses independently of the presence of NKT cells. We conclude that anti-Ly9 mAbs are able to down-modulate antigen-induced antibody responses independently of antigen type.

In vivo anti-Ly9 treatment induces a down-regulation in the expression of the CD19 co-receptor complex and several adhesion molecules

The observation that anti-Ly9 treatment had an effect on the T-D responses, which were not altered in Ly9-deficient mice, prompted us to analyze the consequence of antibody treatment on the remaining FO B cells. First, we assessed the expression of different cell surface molecules on spleen B cells ($B220^+$) after *in vivo* treatment with Ly9.7.144. Anti-Ly9 administration decreased surface protein levels of the B cell co-receptor complex formed by CD19, CD21 and CD81 (Fig. 7A, 7B). This significant reduction was selective, as the levels of other B cell surface proteins such as B220, IgM, and IgD were not significantly affected after treatment (Fig. 7A, 7B). Other cell surface molecules such as CD1d, CD2, CD20, CD22, CD23, CD24, CD38, CD40 CD44, CD45, CD79b and CD84 were not affected or only minimally altered (data not shown). These effects were detected 24 hours after administering anti-Ly9 (Fig. 7A, 7B), and were maintained over 26 days after a single injection of antibody (data not shown). Ly9.7.144 also down-modulated the expression of several adhesion molecules such as CD62L, integrin beta 7, integrin alpha 4, and CD18 on $B220^+$ lymphocytes (Fig. 7C). In contrast, anti-Ly9 treatment did not alter the surface levels of other molecules involved in B cell adhesion and migration such as S1P1 or CXCR5 (Fig. 7C).

Impaired B cell survival, proliferation, and differentiation in anti-Ly9 treated mice

As anti-Ly9 administration reduced the surface expression of the CD19 co-receptor complex, which is critical for B cell activation, we next sought to determine if B cell viability, proliferation and differentiation were impaired after treatment. To this end, 24h after *in vivo* administration of Ly9.7.144 or an isotype control antibody, spleen cells were CFSE-labelled and cultured *ex vivo* over 72h in the presence of LPS or anti-IgM. A significant reduction in cell viability was observed in all culture conditions, as judged by percentage of Live/Dead® positive cells (Fig. 7D). The proliferation of anti-Ly9 treated B cells was significantly impaired, especially after LPS stimulation (Fig. 7E). Moreover, LPS-

induced IgG production was reduced (Fig. 7F). Taken together, these data suggest that anti-Ly9 treatment has an important impact on B cell activation.

Ly9 antibody-mediated functions are Fc-independent

In most cases the effects of mAbs are mediated by their Fc region through the interaction with complement or Fc receptors. To evaluate this possibility, we compared the effect on B cell subsets of anti-Ly9 mAb $F(ab')_2$ fragments with that of the intact antibody. As shown in Fig. 8, $F(ab')_2$ fragments were equally efficient in deleting MZ and B1 B cells (Fig. 8A–C), reducing TI-2 antibody responses (Fig. 8D) and down-modulating the CD19 co-receptor complex (Fig. 8E). These results exclude a role of complement activation or antibody-dependent cell-mediated cytotoxic reaction (ADCC) as a mechanism explaining these anti-Ly9 effects.

Discussion

In this study, we provide evidence that the absence of the cell-surface receptor Ly9 induces a selective expansion of splenic MZ and B1 cells without affecting the development of conventional B cells or myeloid cells. These two subsets of innate-like B cells are primarily involved in rapid Ab production to TI-2 Ags. These antigens are largely associated with extrafollicular B cell responses and represent a powerful first line of defence against pathogens entering the spleen (3, 20). Consistent with this, Ly9-deficient mice showed an increased production of IgG2a, IgG2b and IgG3 against TI-2 antigens (TNP_{65}-Ficoll).

Mice deficient in several cell-surface molecules known to positively regulate B cell antigen receptor (BCR) signalling, such as CD19 or the B cell-activating factor receptor (BAFF-R), present reduced MZ and B1 cells numbers (21–23). In contrast, the opposite phenotype, an increase in the MZ and B1 cell compartment and an enhanced response to T-independent antigens, is observed upon transgenic overexpression of these two stimulatory molecules (24, 25). However, little is known about the cell-surface molecules that negatively regulate the homeostasis of innate-like B cells. Mice deficient in cell-surface molecules that negatively regulate BCR signalling such as CD22, Siglec G, or CD72 do not show an expansion of MZ B cells (26, 27). These mice present alterations in the activation and development of conventional B cells or increased numbers of B1 cells in both spleen and peritoneum. This is clearly different from what we observe in mice lacking Ly9.

The regulation on innate-like B cell homeostasis is especially relevant as the activation of these cells requires a tight regulation since they have very low activation thresholds, and are known to produce polyreactive antibodies that are potentially self-reactive (28). Moreover, since these cells are potent responders to microbial antigen, they may also cause collateral tissue injury (29). Importantly, the expansion of MZ and B1 cells has been associated with autoimmune disorders and malignancy in both mice and humans (21, 30, 31). In the NOD mouse strain, splenic MZ B cells expansion correlates with the development of type 1 diabetes (32, 33). An enlarged MZ B cell pool is also found in different mouse models of Sjögren's syndrome (29, 34–36). In BAFF transgenic mice, MZ-like B cells infiltrate the salivary glands and are thought to contribute to tissue damage (34). Consistent with these observations, we have recently reported that aged Ly9-deficient mice spontaneously develop

features of systemic autoimmunity. Here, we show that young Ly9-deficient mice presented a striking increase in natural antibodies of the IgG3 isotype. Natural antibodies, which recognize multiple conserved microbial epitopes, are mainly produced by MZ and B1a cells and present an important autoimmune potential (37).

MZ cells survival and antibody responses are influenced by their interaction with myeloid and stromal populations in the spleen. The frequency of main myeloid subsets and the distribution of MZ macrophages and adhesion molecules were not altered in Ly9 absence. Furthermore, Ly9$^{-/-}$ mice showed selectively increased antibody responses against TNP-Ficoll, which is able to trigger antibody production by B lymphocytes without T cell help. Collectively, these data supports the idea that Ly9 restrains the size of MZ and B1 cell subsets and regulates the extent of TI-2 responses in a B cell-intrinsic manner. Nevertheless, further experiments will be required to confirm the B cell-autonomous nature of the innate-like B cell expansion and enhanced antibody production observed in Ly9$^{-/-}$ mice.

SLAMF receptors have been shown to modulate lymphocyte function by recruiting activating and inhibitory SH2 domain-containing proteins to immunoreceptor tyrosine-based switch motifs (ITSMs) present in their cytoplasmic tails (6, 7, 38). In cells lacking SAP, such as B cells, tyrosine phosphatases can bind to the ITSMs and transmit negative activation signals (39). Here, we hypothesize that the homophilic interactions of the Ly9 receptor established between adjacent B cells prevent the spontaneous activation of these innate-like B cells by recruiting SHP-2 and SHIP tyrosine-phosphatases (15, 16). These phosphatases are responsible for the negative signals transmitted by most inhibitory co-receptor molecules (40). Together, the phenotype of the Ly9-deficient mice suggests that Ly9 negatively regulates innate-like B lymphocyte activation and homeostasis.

We next decided to study the *in vivo* capacity of a mAb against Ly9 to affect innate-like B cell homeostasis and activation, since this could be a potential approach for treating B cell related diseases. We found that injecting mice with Ly9 mAb resulted in the complete deletion of MZ B cells. It is not clear whether this antibody treatment leads to MZ B cell death or to their migration to other sites. We could not observe the migration of MZ B cells to the blood, as has been observed after treatment with anti-VLA4 mAbs (41). Moreover, the expression of S1P1R and CXCR5, which are known to regulate MZ B cell localization in MZ and migration into follicles, was not altered in the anti-Ly9 treated mice (42–43). We cannot completely exclude the possibility that these cells have changed their phenotype. However, this is highly unlikely, since the deletion of MZ B cells was confirmed using an alternative combination of markers.

Splenic B1 cell numbers were also reduced after antibody treatment, albeit to a lesser extent. However, the numbers of B1 cells in the peritoneum were not affected. Interestingly, the resistance of B cells in the mouse peritoneal cavity has also been reported during CD20 immunotherapy in mice (44). Reduced numbers of T1 cells could be observed only after prolonged anti-Ly9 treatment, but not 24 h after administration of the mAb. Notably, the B cell subsets that were eliminated or reduced by anti-Ly9 treatment (MZ, B1 and T1 cells) are the ones we found expanded in the Ly9-deficient mice. This supports the notion that Ly9.7.144 mAb has an agonistic effect. Furthermore, anti-Ly9 treatment diminished

circulating levels of IgG and IgM, and this decrease was concomitant with a reduction in the numbers of bone marrow plasma cells.

A key finding of our study was that treating animals with Ly9 mAb reduced the *in vivo* production of antibodies not only against TI-2 Ags, but also against TI-1 and T-D Ags. The reduction of T-D humoral responses was independent of the effect of Ly9.7.144 over NKT cells. This therefore demonstrates that Ly9 mAb treatment can reduce Ab production by both innate-like and conventional B cells. This is consistent with our observation that Ly9 treatment caused a reduction in B cell survival, proliferation and differentiation. The ability of anti-Ly9 mAb to hinder humoral immune responses could be a promising therapeutic option in diseases involving the pathogenic production of antibodies (45).

Analysis of a large panel of cell-surface molecules showed that anti-Ly9 treatment induced a fast and selective reduction of the CD19 complex expression, without significantly affecting the levels of molecules that constitute the BCR (IgM, IgD and CD79b) or other B cell associated molecules. This is a surprising result since other B cell-directed treatments, such as CD22, induce a reduction not only of CD19 and CD21, but also of IgM, CD79b, or CD20 (46). Moreover, the effect of CD22 Abs was mediated by a Fc/FcR-dependent membrane transfer from B cells to effector cells via trogocytosis, whereas the reduction of the CD19 complex induced by anti-Ly9 injection is not only more selective, but also Fc-independent (46). The observation that the anti-Ly9 mediated effects are Fc-independent also excludes the possible participation of complement system or ADCC in the observed phenotype. Although more experiments are required to explain the mechanism of action of anti-Ly9 Abs, a down-modulation in the expression of the CD19 complex may represent the main molecular mechanism responsible for the alterations in B cell subsets and humoral response deficiency observed in the treated mice. No alteration in the expression of the CD19 complex could be observed in the Ly9-deficient mice. Thus, we hypothesize that the wide-ranging effect of the anti-Ly9 as compared to the phenotype of the Ly9-defcient mice is potentially due to an impairment in the CD19 dependent signaling that affects the function of the conventional B cells. The CD19 complex is critical for B cell activation and the homeostasis of MZ and B1 cells by modulating signal transduction through the BCR or by inducing survival tonic signals (47). Moreover, elevated CD19 has been correlated with susceptibility to autoimmunity in both mice and humans (48, 49).

In contrast to B cell antibody depletion therapies, inhibition of signalling pathways and selective elimination of MZ and B1 cells with minimal reduction of the conventional B cell compartment should be regarded as a promising new therapeutic option.

Supplementary Material

Refer to Web version on PubMed Central for supplementary material.

Acknowledgments

We thank A. Lázaro and I. Azagra for technical assistance.

Abbreviations used in this article

BTK	Bruton's tyrosine kinase
CXCR5	chemokine (C-X-C Motif) receptor 5
FO	follicular
ICAM-1	Intercellular Adhesion Molecule-1
KLH	keyhole limpet hemocyanin
MFI	mean fluorescence intensity
MZ	marginal zone
S1P1	sphingosine 1-phosphate receptor 1
SIGN-R1	specific intracellular adhesion molecule-grabbing nonintegrin receptor-1
SLAM	signaling lymphocytic activation molecule
T1	transitional 1
T-D	T-Dependent
TI-1 and TI-2	T-Independent 1 and 2
TNP	2,4,6-trinitrophenyl
VCAM-1	vascular cell adhesion molecule-1
WT	wild-type

References

1. Martin F, Kearney JF. Marginal-zone B cells. Nat Rev Immunol. 2002; 2:323–335. [PubMed: 12033738]
2. Zouali M, Richard Y. Marginal zone B-cells, a gatekeeper of innate immunity. Front Immunol. 2011; 2:63. [PubMed: 22566852]
3. Martin F, Oliver AM, Kearney JF. Marginal zone and B1 B cells unite in the early response against T-independent blood-borne particulate antigens. Immunity. 2001; 14:617–629. [PubMed: 11371363]
4. Lopes-Carvalho T, Foote J, Kearney JF. Marginal zone B cells in lymphocyte activation and regulation. Curr Opin Immunol. 2005; 17:244–250. [PubMed: 15886113]
5. Cerutti A, Cols M, Puga I. Marginal zone B cells: virtues of innate-like antibody-producing lymphocytes. Nat Rev Immunol. 2013; 13:118–132. [PubMed: 23348416]
6. Engel P, Eck MJ, Terhorst C. The SAP and SLAM families in immune responses and X-linked lymphoproliferative disease. Nat Rev Immunol. 2003; 3:813–821. [PubMed: 14523387]
7. Cannons JL, Tangye SG, Schwartzberg PL. SLAM family receptors and SAP adaptors in immunity. Annu Rev Immunol. 2011; 29:665–705. [PubMed: 21219180]
8. Veillette A, Dong Z, Latour S. Consequence of the SLAM-SAP signaling pathway in innate-like and conventional lymphocytes. Immunity. 2007; 27:698–710. [PubMed: 18031694]
9. Romero X, Sintes J, Engel P. Role of SLAM Family Receptors and Specific Adapter SAP in Innate-Like Lymphocytes. Crit Rev Immunol. 2014; 34:263–299. [PubMed: 24941157]
10. de la Fuente MA, Tovar V, Villamor N, Zapater N, Pizcueta P, Campo E, Bosch J, Engel P. Molecular characterization and expression of a novel human leukocyte cell-surface marker homologous to mouse Ly-9. Blood. 2001; 97:3513–3520. [PubMed: 11369645]

11. Sintes J, Vidal-Laliena M, Romero X, Tovar V, Engel P. Characterization of mouse CD229 (Ly9), a leukocyte cell surface molecule of the CD150 (SLAM) family. Tissue Antigens. 2007; 70:355–362. [PubMed: 17919264]
12. Zucchetto A, Cattarossi I, Nanni P, Zaina E, Prato G, Gilestro M, Marconi D, Bulian P, Rossi FM, Del Vecchio L, Omedè P, Geuna M, Del Poeta G, Gattei V. Cluster analysis of immunophenotypic data: the example of chronic lymphocytic leukemia. Immunol Lett. 2011; 134:137–144. [PubMed: 20923685]
13. Atanackovic D, Panse J, Hildebrandt Y, Jadczak A, Kobold S, Cao Y, Templin J, Meyer S, Reinhard H, Bartels K, Lajmi N, Zander AR, Marx AH, Bokemeyer C, Kröger N. Surface molecule CD229 as a novel target for the diagnosis and treatment of multiple myeloma. Haematologica. 2011; 96:1512–1520. [PubMed: 21606160]
14. Romero X, Zapater N, Calvo M, Kalko SG, de la Fuente MA, Tovar V, Ockeloen C, Pizcueta P, Engel P. CD229 (Ly9) lymphocyte cell surface receptor interacts homophilically through its N-terminal domain and relocalizes to the immunological synapse. J Immunol. 2005; 174:7033–7042. [PubMed: 15905546]
15. Sayós J, Martín M, Chen A, Simarro M, Howie D, Morra M, Engel P, Terhorst C. Cell surface receptors Ly-9 and CD84 recruit the X-linked lymphoproliferative disease gene product SAP. Blood. 2001; 97:3867–3874. [PubMed: 11389028]
16. Li C, Iosef C, Jia CY, Han VK, Li SS. Dual functional roles for the X-linked lymphoproliferative syndrome gene product SAP/SH2D1A in signaling through the signaling lymphocyte activation molecule (SLAM) family of immune receptors. J Biol Chem. 2003; 278:3852–3859. [PubMed: 12458214]
17. Sintes J, Cuenca M, Romero X, Bastos R, Terhorst C, Angulo A, Engel P. Cutting edge: Ly9 (CD229), a SLAM family receptor, negatively regulates the development of thymic innate memory-like CD8+ T and invariant NKT cells. J Immunol. 2013; 190:21–26. [PubMed: 23225888]
18. de Salort J, Cuenca M, Terhorst C, Engel P, Romero X. Ly9 (CD229) Cell-Surface Receptor is Crucial for the Development of Spontaneous Autoantibody Production to Nuclear Antigens. Front Immunol. 2013; 4:225. [PubMed: 23914190]
19. Graham DB, Bell MP, McCausland MM, Huntoon CJ, van Deursen J, Faubion WA, Crotty S, McKean DJ. Ly9 (CD229)-deficient mice exhibit T cell defects yet do not share several phenotypic characteristics associated with SLAM- and SAP-deficient mice. J Immunol. 2006; 176:291–300. [PubMed: 16365421]
20. Fagarasan S, Honjo T. T-Independent immune response: new aspects of B cell biology. Science. 2000; 290:89–92. [PubMed: 11021805]
21. Martin F, Kearney JF. Positive selection from newly formed to marginal zone B cells depends on the rate of clonal production, CD19, and btk. Immunity. 2000; 12:39–49. [PubMed: 10661404]
22. You Y, Zhao H, Wang Y, Carter RH. Cutting edge: Primary and secondary effects of CD19 deficiency on cells of the marginal zone. J Immunol. 2009; 182:7343–7347. [PubMed: 19494255]
23. Schiemann B, Gommerman JL, Vora K, Cachero TG, Shulga-Morskaya S, Dobles M, Frew E, Scott ML. An essential role for BAFF in the normal development of B cells through a BCMA-independent pathway. Science. 2001; 293:2111–2114. [PubMed: 11509691]
24. Inaoki M, Sato S, Weintraub BC, Goodnow CC, Tedder TF. CD19-regulated signaling thresholds control peripheral tolerance and autoantibody production in B lymphocytes. J Exp Med. 1997; 186:1923–1931. [PubMed: 9382890]
25. Batten M, Groom J, Cachero TG, Qian F, Schneider P, Tschopp J, Browning JL, Mackay F. BAFF mediates survival of peripheral immature B lymphocytes. J Exp Med. 2000; 192:1453–1466. [PubMed: 11085747]
26. Parnes JR, Pan C. CD72, a negative regulator of B-cell responsiveness. Immunol Rev. 2000; 176:75–85. [PubMed: 11043769]
27. Müller J, Nitschke L. The role of CD22 and Siglec-G in B-cell tolerance and autoimmune disease. Nat Rev Rheumatol. 2014; 10:422–428. [PubMed: 24763061]
28. Bendelac A, Bonneville M, Kearney JF. Autoreactivity by design: innate B and T lymphocytes. Nat Rev Immunol. 2001; 1:177–186. [PubMed: 11905826]

29. Varin MM, Le Pottier L, Youinou P, Saulep D, Mackay F, Pers JO. B-cell tolerance breakdown in Sjögren's syndrome: focus on BAFF. Autoimmun Rev. 2010; 9:604–608. [PubMed: 20457281]
30. Mandik-Nayak L, Racz J, Sleckman BP, Allen PM. Autoreactive marginal zone B cells are spontaneously activated but lymph node B cells require T cell help. J Exp Med. 2006; 203:1985–1998. [PubMed: 16880262]
31. Viau M, Zouali M. B-lymphocytes, innate immunity, and autoimmunity. Clin Immunol. 2005; 114:17–26. [PubMed: 15596405]
32. Mariño E, Batten M, Groom J, Walters S, Liuwantara D, Mackay F, Grey ST. Marginal-zone B-cells of nonobese diabetic mice expand with diabetes onset, invade the pancreatic lymph nodes, and present autoantigen to diabetogenic T-cells. Diabetes. 2008; 57:395–404. [PubMed: 18025414]
33. Stolp J, Mariño E, Batten M, Sierro F, Cox SL, Grey ST, Silveira PA. Intrinsic molecular factors cause aberrant expansion of the splenic marginal zone B cell population in nonobese diabetic mice. J Immunol. 2013; 191:97–109. [PubMed: 23740954]
34. Groom J, Kalled SL, Cutler AH, Olson C, Woodcock SA, Schneider P, Tschopp J, Cachero TG, Batten M, Wheway J, Mauri D, Cavill D, Gordon TP, Mackay CR, Mackay F. Association of BAFF/BLyS overexpression and altered B cell differentiation with Sjögren's syndrome. J Clin Invest. 2002; 109:59–68. [PubMed: 11781351]
35. Nguyen CQ, Kim H, Cornelius JG, Peck AB. Development of Sjogren's syndrome in nonobese diabetic-derived autoimmune-prone C57BL/6.NOD-Aec1Aec2 mice is dependent on complement component-3. J Immunol. 2007; 179:2318–2329. [PubMed: 17675493]
36. Qian Y, Giltiay N, Xiao J, Wang Y, Tian J, Han S, Scott M, Carter R, Jorgensen TN, Li X. Deficiency of Act1, a critical modulator of B cell function, leads to development of Sjögren's syndrome. Eur J Immunol. 2008; 38:2219–2228. [PubMed: 18624351]
37. Vas J, Grönwall C, Silverman GJ. Fundamental roles of the innate-like repertoire of natural antibodies in immune homeostasis. Front Immunol. 2013; 4:4. [PubMed: 23386848]
38. Ma CS, Deenick EK. The role of SAP and SLAM family molecules in the humoral immune response. Ann N Y Acad Sci. 2011; 1217:32–44. [PubMed: 21091715]
39. Kageyama R, Cannons JL, Zhao F, Yusuf I, Lao C, Locci M, Schwartzberg PL, Crotty S. The receptor Ly108 functions as a SAP adaptor-dependent on-off switch for T cell help to B cells and NKT cell development. Immunity. 2012; 36:986–1002. [PubMed: 22683125]
40. Tsubata T. Role of inhibitory BCR co-receptors in immunity. Infect Disord Drug Targets. 2012; 12:181–190. [PubMed: 22394175]
41. Lu TT, Cyster JG. Integrin-mediated long-term B cell retention in the splenic marginal zone. Science. 2002; 297:409–412. [PubMed: 12130787]
42. Cinamon G, Matloubian M, Lesneski MJ, Xu Y, Low C, Lu T, Proia RL, Cyster JG. Sphingosine 1-phosphate receptor 1 promotes B cell localization in the splenic marginal zone. Nat Immunol. 2004; 5:713–720. [PubMed: 15184895]
43. Cinamon G, Zachariah MA, Lam OM, Foss FW Jr, Cyster JG. Follicular shuttling of marginal zone B cells facilitates antigen transport. Nat Immunol. 2008; 9:54–62. [PubMed: 18037889]
44. Hamaguchi Y, Uchida J, Cain DW, Venturi GM, Poe JC, Haas KM, Tedder TF. The peritoneal cavity provides a protective niche for B1 and conventional B lymphocytes during anti-CD20 immunotherapy in mice. J Immunol. 2005; 174:4389–4899. [PubMed: 15778404]
45. Engel P, Gómez-Puerta JA, Ramos-Casals M, Lozano F, Bosch X. Therapeutic targeting of B cells for rheumatic autoimmune diseases. Pharmacol Rev. 2011; 63:127–156. [PubMed: 21245206]
46. Rossi EA, Goldenberg DM, Michel R, Rossi DL, Wallace DJ, Chang CH. Trogocytosis of multiple B-cell surface markers by CD22 targeting with epratuzumab. Blood. 2013; 122:3020–3029. [PubMed: 23821660]
47. Haas KM, Tedder TF. Role of the CD19 and CD21/35 receptor complex in innate immunity, host defense and autoimmunity. Adv Exp Med Biol. 2005; 560:125–139. [PubMed: 15934172]
48. Sato S, Hasegawa M, Fujimoto M, Tedder TF, Takehara K. Quantitative genetic variation in CD19 expression correlates with autoimmunity. J Immunol. 2000; 165:6635–6643. [PubMed: 11086109]

49. Nicholas MW, Dooley MA, Hogan SL, Anolik J, Looney J, Sanz I, Clarke SH. A novel subset of memory B cells is enriched in autoreactivity and correlates with adverse outcomes in SLE. Clin Immunol. 2008; 126:189–201. [PubMed: 18077220]

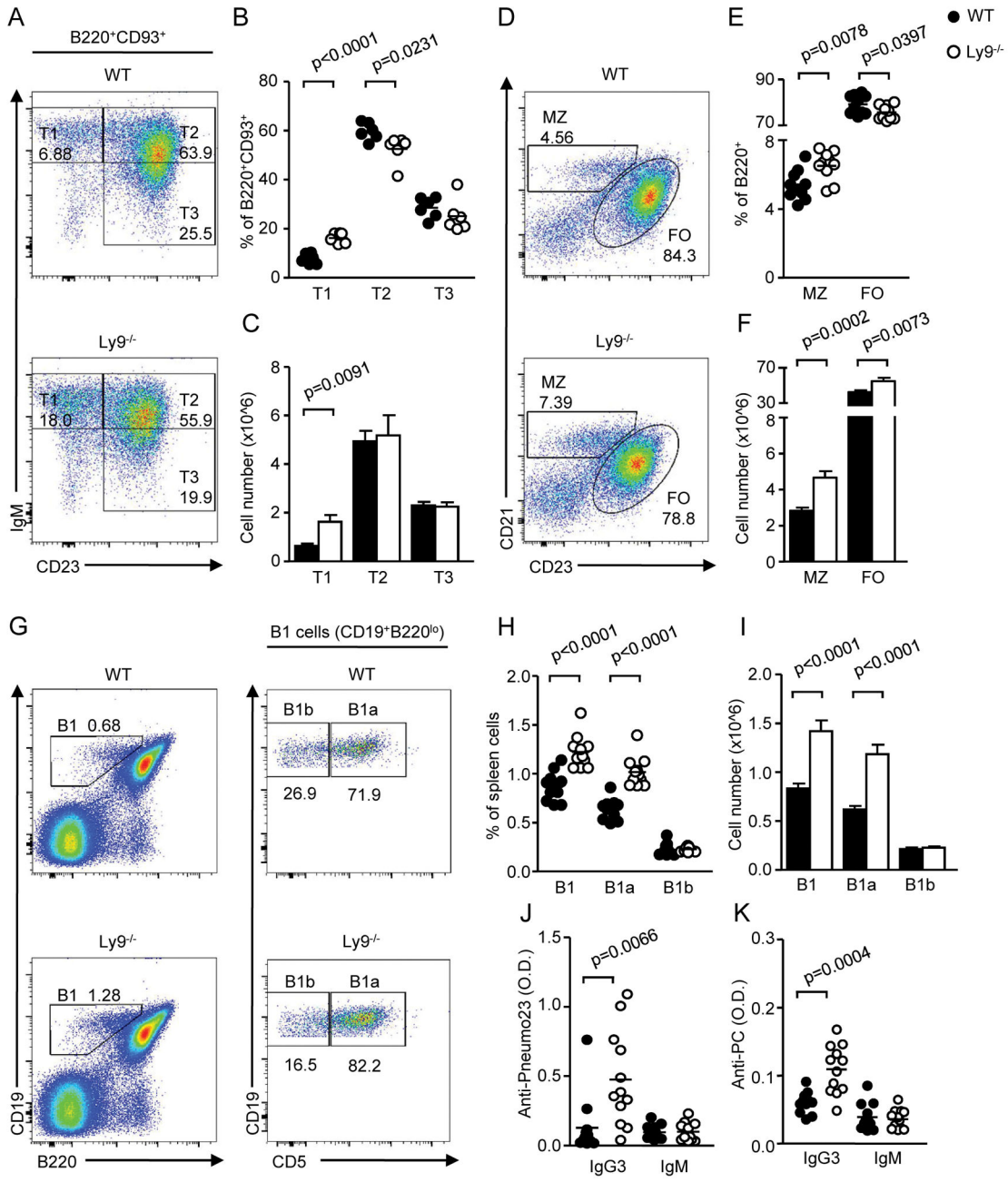

Figure 1. Increased proportions of T1, MZ, and B1 B cells and enhanced levels of natural antibodies in *Ly9*-deficient mice

(A) Representative staining of transitional 1 (IgM^{hi} $CD23^{lo}$), transitional 2 (IgM^{hi} $CD23^{hi}$), and transitional 3 (IgM^{lo} $CD23^{hi}$) spleen cells in gated $B220^{hi}$ $CD93^{hi}$ lymphocytes. (B) Cumulative data of percentages and (C) absolute cell numbers of T1, T2 and T3 cells in WT and $Ly9^{-/-}$ mice. (D) Spleen marginal zone (MZ; $CD21^{hi}$ $CD23^{lo}$) and follicular (FO; $CD21^{lo}$ $CD23^{hi}$) B cell proportions in gated $B220^{+}$ cells from mice of the indicated genotypes. (E) Cumulative data of frequencies and (F) absolute cell numbers of MZ and FO cells in WT and $Ly9^{-/-}$ mice. (G) Spleen lymphocytes from WT and $Ly9^{-/-}$ mice were

stained for CD19, B220, and CD5. Representative dot plot histograms showing B1 ($CD19^{hi}$ $B220^{lo}$) cell frequency, and further division into B1a ($CD5^{+}$) and B1b ($CD5^{-}$) subsets. (H) Cumulative data of percentages and (I) absolute numbers of splenic B1, B1a and B1b cells in WT and $Ly9^{-/-}$ mice. (J–K) Levels of IgG3 and IgM natural antibodies reactive to (J) *S. pneumoniae* capsular polysaccharides (Pneumo23® vaccine) and to (K) phosphorylcholine (PC) in the serum of naive WT and $Ly9^{-/-}$ mice. Symbols represent individual mice. Results are expressed as optical density (OD) values at 405 nm. Data are representative of at least two independent experiments with 4 to 6 mice per group.

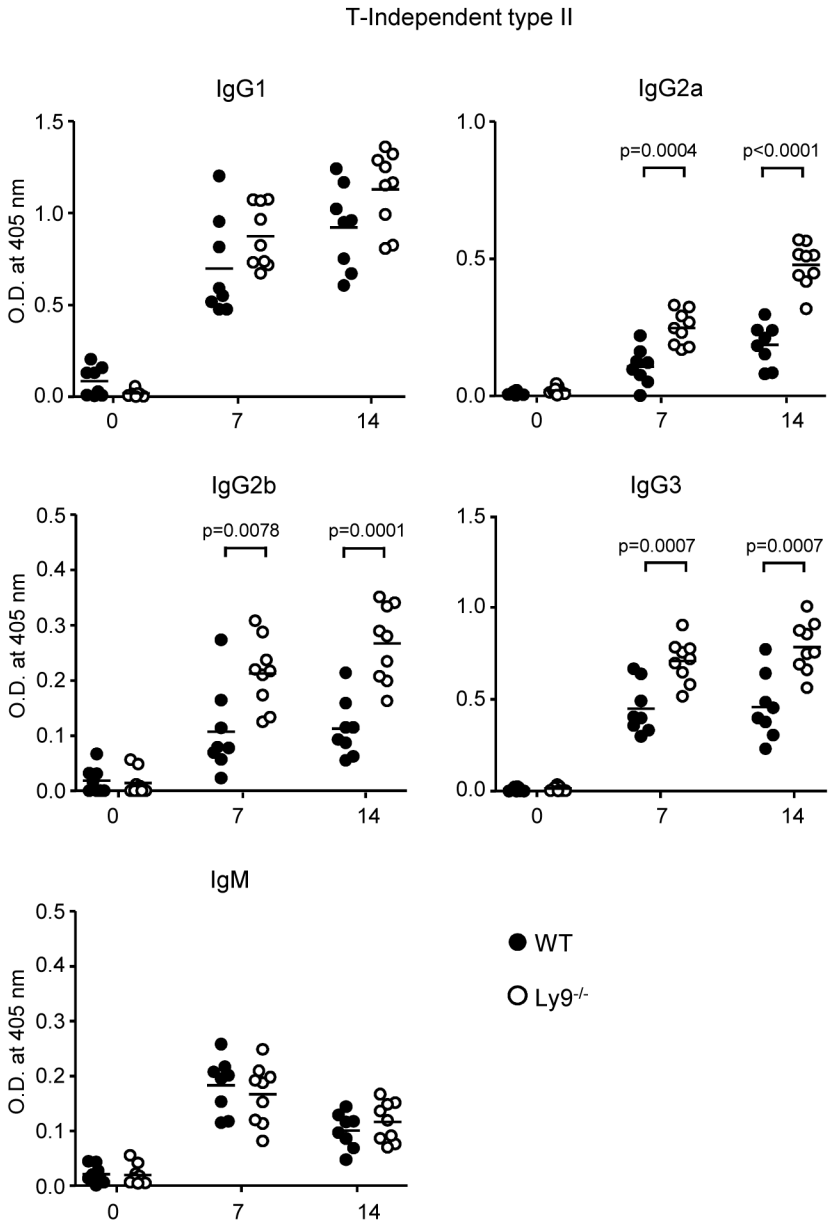

Figure 2. Ly9 absence leads to enhanced B cell antibody responses against T-Independent type II antigens

Determination of anti-TNP specific antibody levels in the serum from 10-week-old WT and $Ly9^{-/-}$ mice. Animals were immunized intraperitoneally with TNP_{65}-Ficoll on day 0 and bled on days 7 and 14. Results are expressed as optical density (OD) values at 405 nm. Data are from two independent experiments with four to five mice per group.

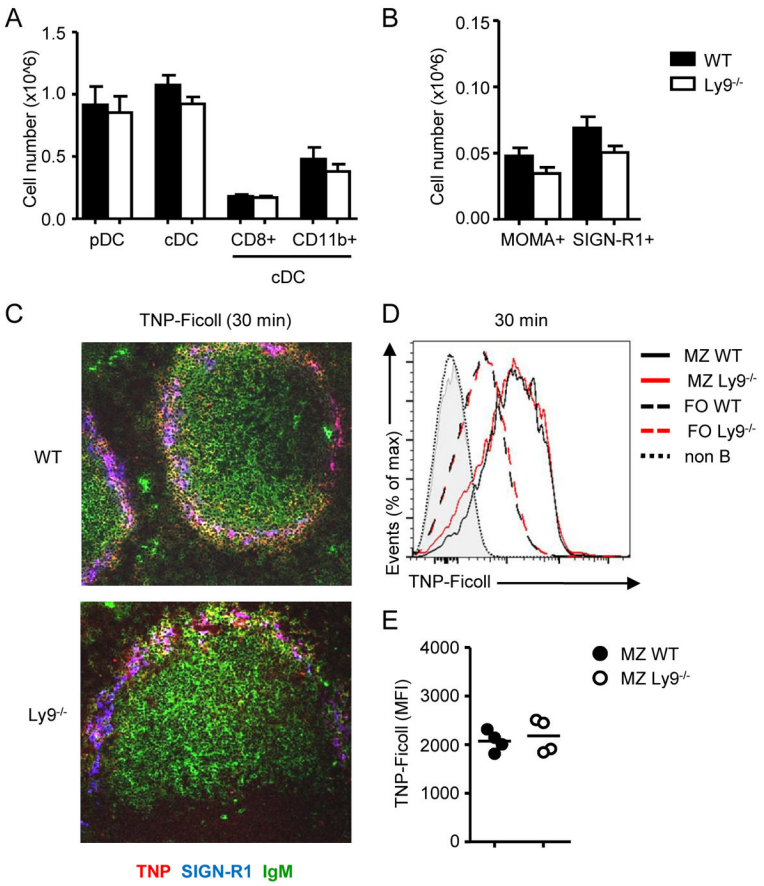

Figure 3. Myeloid cells and T-independent antigen capture are not altered in Ly9 deficient mice

(A) Absolute numbers of pDCs ($B220^+$ $CD11c^+$), cDCs ($B220^-$ MHC^-II^+ $CD11c^+$), $CD8^+$ cDCs ($CD8^+$ $CD11b^-$), $CD11b^+$ cDCs ($CD8^-$ $CD11b^+$) and (B) numbers of metallophilic ($CD11b^+$ $MOMA\text{-}1^+$) and MZ ($CD11b^+$ $SIGN\text{-}R1^+$) macrophages in spleens from WT and $Ly9^{-/-}$ mice. Data shown are mean ± SEM of eight animals. (C) TNP uptake in WT and $Ly9^{-/-}$ MZ 30 minutes after i.v administration of 50 μg TNP-Ficoll. 5 μm frozen spleen sections were stained with anti-TNP (red), anti-SIGN-R1 (blue) and anti-IgM (green) antibodies and analysed by confocal microscopy. Image magnification 20x. (D) Representative histograms of bound TNP in MZ or follicular B cells from WT (n=4) or $Ly9^{-/-}$ (n=4) mice. (E) Mean fluorescence intensity of captured TNP in MZ B cells. Each dot represents an individual mouse. Data are representative of at least two independent experiments.

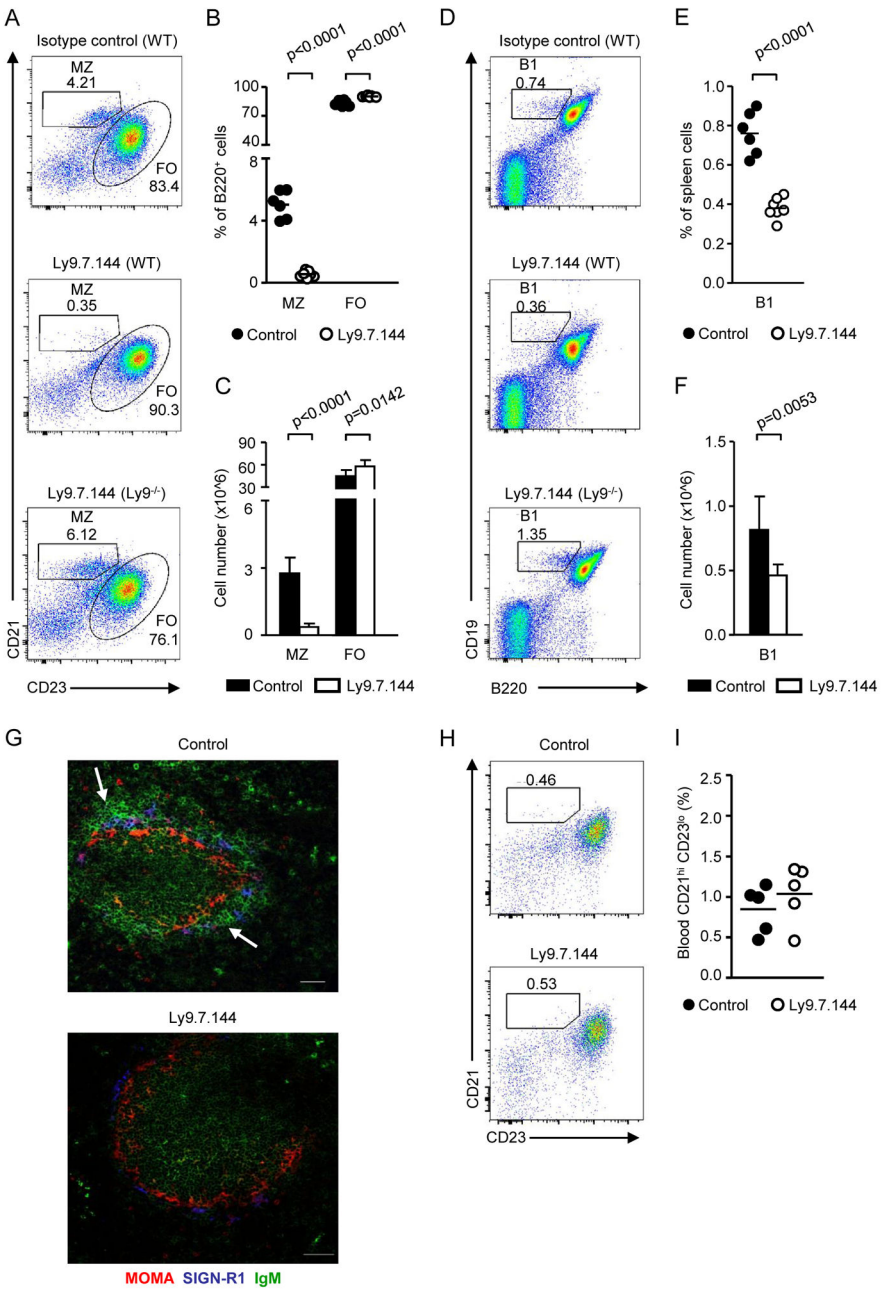

Figure 4. Administering anti-Ly9 specifically depletes splenic MZ and B1 B cells in WT mice

Analysis of B cell subsets in spleen and blood 24h after treatment of WT mice with Ly9.7.144 or an isotype matching antibody. (A) Representative dot plot histograms of spleen cells from mice of the indicated genotypes stained with B220, CD21, and CD23 mAbs. (B) Frequencies and (C) absolute cell numbers of marginal zone and follicular B cell subsets 24h after Ly9.7.144 treatment. (D) Flow cytometric analysis of spleen B1 cells from treated WT and Ly9$^{-/-}$ mice. (E) Cumulative data of percentages and (F) absolute numbers of splenic B1 cells after anti-Ly9 administration. (G) Spleen cryosections from WT mice 24h after injection with control antibody (left) or Ly9.7.144 (right). 5 μm frozen sections were

stained with antibodies against MOMA (red), SIGN-R1 (blue) and IgM (green), and analysed by confocal microscopy. White arrows indicate areas rich in MZ B cells, which could not be detected in anti-Ly9 treated mice. Images are 1 μm confocal pictures captured as described in the “Tissue staining and confocal microscopy” section, and are representative of each group. Image magnification 20x. Scale bars, 50 μm. (H) Flow cytometric analysis of blood $B220^{+}$ cells in mice 24h after administration of Ly9.7.144 (n=5) or a control antibody (n=5). (I) Frequency of $CD21^{hi}$ $CD23^{lo}$ cells in blood after treatment. Data are representative of three (A–G) or two (H–I) independent experiments with three to four mice per group.

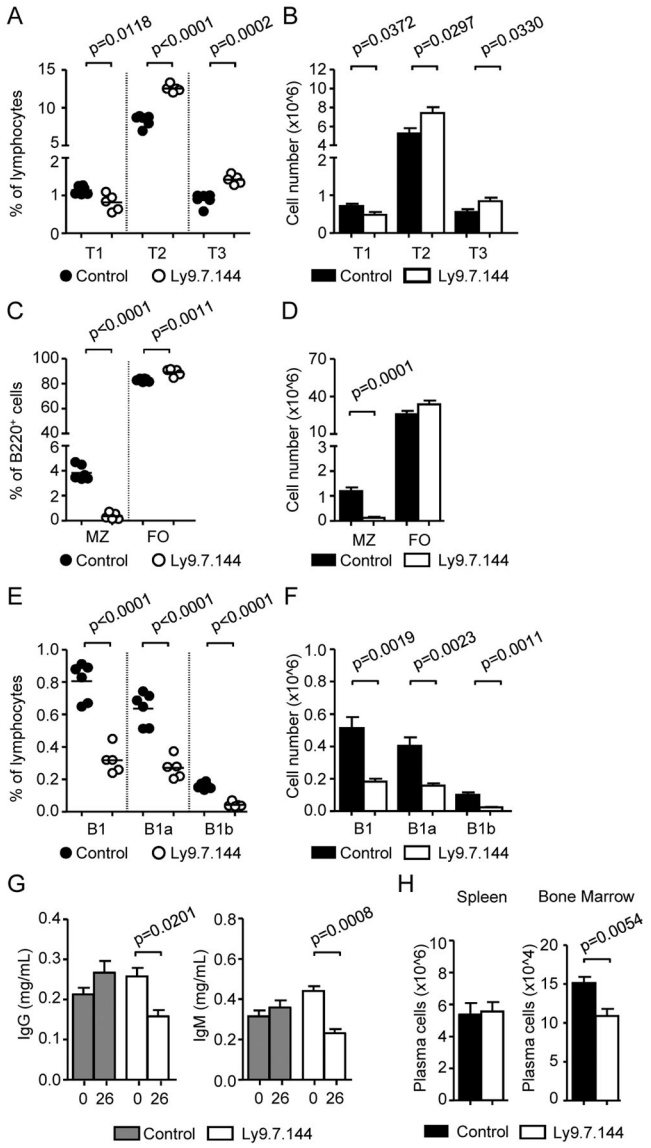

Figure 5. Anti-Ly9 mediated depletion of marginal zone and B1 B cells is maintained long-term after a single administration

Mice (n=5/group) received 250 μg of Ly9.7.144 or control antibody i.p. on day 0. 26 days later, mice were sacrificed and spleen subsets were analysed by flow cytometry. (A) Proportion and (B) absolute cell numbers of transitional T1, T2 and T3 cells in spleens from anti-Ly9 or control treated mice. (C) Percentage and (D) absolute cell numbers of MZ and FO B subsets. (E) Frequencies and (F) cell numbers of spleen B1, B1a and B1b cells. (G) Total levels of IgG (left) and IgM (right) in mice serum before being treated (day 0) or 26 days after receiving a single dose of either control mAb or Ly9.7.144. Statistical significance was determined using a two-tailed paired Student's *t* test. (H) Absolute cell number of $B220^{int}$ $CD138^{+}$ plasma cells in the spleen (left) and bone marrow (right) of control or anti-Ly9 treated animals. Data are representative of two independent experiments.

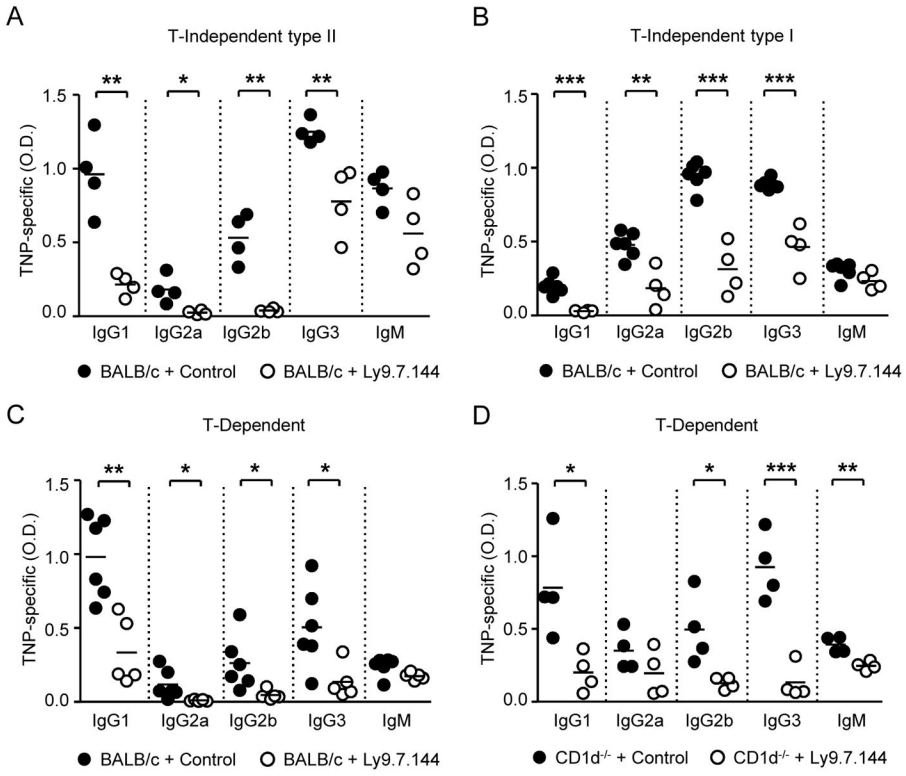

Figure 6. Anti-Ly9 treatment significantly diminishes antibody production against both T-Independent and T-Dependent antigens

TNP-specific antibody levels in serum from mice treated with anti-Ly9 or control antibody. Animals (n=4–6/ group) received a single i.p. dose (250 μg) of Ly9.7.144 or an isotype-matching mAb 24h before immunization. (A) Anti-TNP specific antibody levels 7 days after immunization with 50 μg TNP_{65}-Ficoll, (B) 11 days after immunization with 50 μg $TNP_{0.3}$-LPS, or (C) 9 days after immunization with 100 μg TNP_{31}-KLH. (D) Levels of anti-TNP specific antibodies in pretreated $CD1d^{-/-}$ mice 9 days after immunization with 100 μg TNP_{31}-KLH. Symbols represent individual mice. Results are expressed as optical density (OD) values at 405 nm. Statistical significances are shown (*, $p<0.05$; **, $p<0.01$; ***, $p<0.001$).

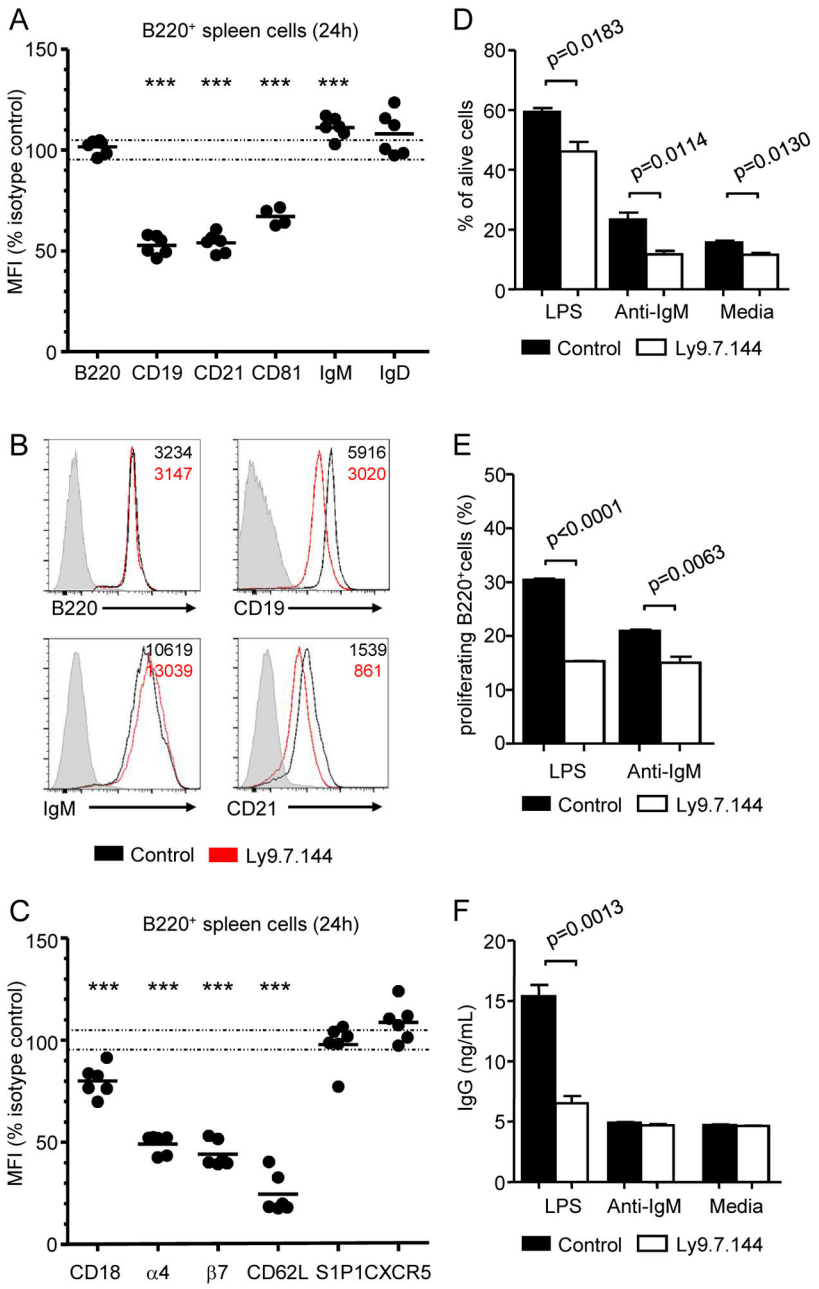

Figure 7. Anti-Ly9 treatment decreases surface expression of B cell co-receptor associated molecules, and impairs B cell proliferation, survival and antibody production

(A) Relative mean fluorescence intensity (MFI) of the indicated surface molecules in spleen B lymphocytes 24 hours after *in vivo* administration of Ly9.7.144. Each dot represents the % over the mean MFI of the control group. (B) Representative histograms showing surface expression of B220, CD19, IgM and CD21 in $B220^+$ spleen cells from either anti-Ly9 or control mAb-treated mice. Numbers in quadrants indicate the MFI of $B220^+$ cells from control (black) or Ly9.7.144 treated (red) mice. (C) Relative MFI (% over the mean MFI of the control group) of the indicated adhesion molecules in $B220^+$ cells 24h after treatment with Ly9.7.144. (D–F) Ly9 mAb treatment impairs B cell *ex vivo* viability, proliferation, and

differentiation. WT mice received 250 μg of Ly9.7.144 or isotype control antibody i.p. 24 hours later, spleen cells were stained with CFSE and cultured in medium alone or in the presence of LPS (10 μg/mL) or $F(ab')_2$ fragments anti-mouse IgM (10 μg/mL. (D) After 72h in culture, percentage of alive (LiveDead® negative) $B220^+$ cells was assessed by flow cytometry. (E) Proliferating B cells ($B220^+$ CFSElow) were identified by flow cytometry after a 72h culture. (F) Total IgG in culture supernatants (72h) was quantified by ELISA. Statistical differences are shown. (A, C) Statistical significance: **, $p<0.001$; ***, $p<0.0001$. Data are representative of three (A–C) or two (D–F) separated experiments with four to five mice per group.

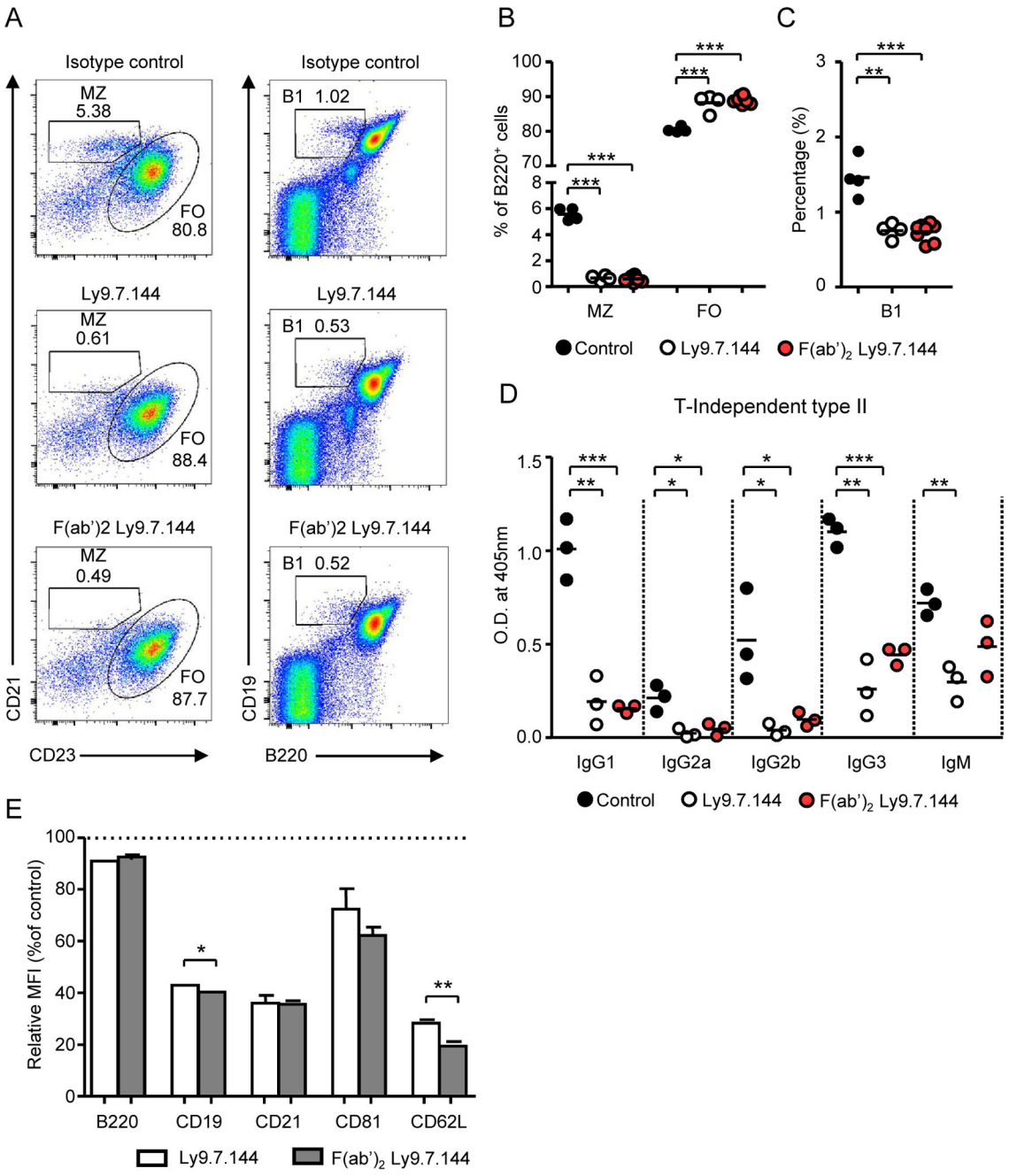

Figure 8. Ly9.7.144 effects are Fc-independent

(A–C) BALB/c mice (n=4–7/ group) received i.p. 50 μg of whole Ly9.7.144, F(ab′)$_2$ Ly9.7.144, or isotype control mAb. 24 hours later, spleen subsets were analysed by FACS. (A) Representative dot plots showing spleen MZ and FO cell compartments (*left panels*) and B1 cell proportions (*right panels*) 24h after treatment. (B) Percentage of MZ, FO and (C) B1 cells 24h after receiving whole anti-Ly9 or F(ab′)$_2$ Ly9.7.144. (D) WT mice (n=3/group) received 50 μg of Ly9.7.144, F(ab′)$_2$ Ly9.7.144, or isotype control mAb i.p. on days 0, 3, and 6. On day 1, mice were immunized i.p. with 50 μg TNP$_{(65)}$Ficoll. On day 8, mice were

sacrificed and anti-TNP specific antibody levels in the serum were determined by ELISA. Results are expressed as optical density (OD) values at 405 nm. (E) Relative MFI (% over the mean MFI of the control group) of the indicated surface molecules in $B220^+$ cells 24h after treatment with 50 μg Ly9.7.144 or $F(ab')_2$ Ly9.7.144.